A Comparison of Global MPPT Techniques for Partially Shaded Grid-connected Photovoltaic System

Afef Badis*, Mohamed Habib Boujmil**‡, Mohamed Nejib Mansouri***

* Electrical Engineering Department, National Engineering School of Monastir (ENIM), University of Monastir, Av. Ibn El Jazzar Skanes (5000), TUNISIA

** Electrical Engineering Department, Higher Institute of Technological Studies of Nabeul, 8000, Nabeul, Tunisia

***Department Electrical Engineering Department, National Engineering School of Monastir (ENIM), University of Monastir, Av. Ibn El Jazzar Skanes (5000), TUNISIA

(badis.afef@gmail.com, mohamedhabib.boujmil@isetn.rnu.tn, mansouri.nejib@hotmail.fr)

‡ Afef Badis, Av. Ibn El Jazzar Skanes (5000), TUNISIA, Phone: +216 73 500 244, badis.afef@gmail.com

Received: 25.04.2018 Accepted:31.05.2018

Abstract- Maximizing the energy reproduced from a solar power generation system becomes a challenging task when high changes in irradiation or Partial Shading (PS) are experienced. The latter case is considered as one of the unavoidable complicated phenomena since the Photovoltaic (PV) system is extremely affected by displaying numerous local maxima. Thus, it is compulsory to rigorously choose an accurate Maximum Power Point Tracking (MPPT) which identifies effectively the unique Global Point (GP) and avoid any local peaks with the purpose of mitigating the impact of PS. Conventional methods are prone to failure in case of an unpredictable shadow. This paper introduces a comparative assessment of Particle Swarm Optimization (PSO) based MPPT, Genetic Algorithm (GA) based MPPT and P&O for a partially shaded grid-connected photovoltaic system. The main contribution of the paper consists in developing a new variant of PSO algorithm which is a good tradeoff between simplicity, speed, and efficiency. The grid side control is investigated as well through developing different control loops with PID controllers tuned by GA. Various schemes of irradiation and PS are used in order to verify the ability of the threefold algorithms to adequately track the GP.

Keywords: MPPT, Particle Swarm Optimization, Partial shading, Genetic Algorithm, Grid-connected PV systems.

Nomenclature:

V_{pv}	PV cell Voltage (V)
I_{pv}	PV cell output current (A)
V_m	Maximum power voltage (V)
I_m	Maximum power current (A)
V_{ocn}	Nominal open circuit voltage (V_{ocn})
I_{scn}	Nominal short circuit current (I_{scn})
V_T	thermal junction voltage (KT/q)
q	Electron charge (C)
N	diode constant
K_V	Voltage/temperature coefficient (V/K)
K_I	current/temperature coefficient (A/K)
K	Boltzman's constant (J/K)
T	temperature (K)
N_s	number of cell series
N_p	number of cells in parallel
ΔT	variation from the nominal temperature
$v_{r1,2,3}$	the grid voltages
$v_{m1,2,3}$	the modulated voltages of inverter
$v_{rd,q}$	the grid voltages in dq reference frame
$v_{md,q}$	the modulated voltages of inverter in the dq reference frame
u_m	the modulated voltage of the boost converter
u_{dc}	DC link voltage
$i_{r1,2,3}$	the grid currents
$i_{rd,q}$	the grid currents in the dq reference frame
i_m	the modulated current of boost converter
i_{rm}	the modulated current of inverter
$c_1=c_2$	the acceleration coefficients;
m_{reg}	the modulation index.

1. Introduction

Solar Photovoltaic (PV) energy is a potential and environmentally friendly resource of energy which has become widely explored till date owing to its omnipresence, availability, free gas emission, and reduced maintenance cost [1]. However, considering the high initial investment on solar PV generation systems, operating at the Maximum Power Point (MPP) should be permanently maintained under any circumstances, especially when solar irradiation and temperature vary or when Partial Shading (PS) occurs. Else ways, important power losses are figured [2],[3].

With no shading, several conventional methods are disclosed in the literature as a good tracker of the MPP, namely Incremental Conductance (IC), Hill Climbing (HC), and Perturb and Observe (P&O) [4],[6]. Though, when the PV Generator suffers from PS, the mission becomes further complicated because of the non-linearity in the PV characteristics which are characterized by only one global point (GP) among many local peaks (LP). In this state, conventional Maximum Power Point Tracking (MPPT) algorithms mostly get trapped into one of the local maxima. In fact, when a PV module is affected by shadow, the power consumption is raised. In such a case, adding a bypass diode in parallel with each series connection of PV cells is required. However, this leads to developing multiple peak power points. That's why a powerful MPPT technique which is capable to reach the GP fast and smoothly is needed [7]. Moreover, the optimal energy transfer to the grid is ensured through developing grid side control loops.

Several papers in the literature proposing new or enhancing already existed MPPT schemes are developed to overcome the above deficiencies. In the late time, computational intelligent algorithms such as artificial neural network [8], and fuzzy logic approach [9] guarantee global convergence in spite of the huge number of neural network data and the computational complexity accordingly. An evolutionary algorithm (EA) based MPPT algorithms seems to be powerful tools for the GP tracking purpose. This fact is evident from several papers, namely Ant colony optimization (ACO) used in [10], Bat Algorithm (BA) proposed in [11], Genetic Algorithm (GA) reported in [12], chaotic search in [13], and cuckoo search [14]. However, the Particle Swarm Optimization (PSO) technique has become a well-known algorithm which successfully alleviates the impact of PS due its good performance. Furthermore, various modifications and combinations have been performed to the standard PSO algorithm in order to enhance the capability of tracking the GP in a simpler and faster way. Indeed, a combined PSO with IC MPPT method is reported in [15]. Conventional MPPT looks for the MPP under uniform irradiation. Otherwise, PSO tracks the global MPP only when the PV generator is subjected to PS. Good results are obtained by using this method in spite of the extensive number of used particles. A novel Deterministic PSO (DPSO) is introduced in [16]. In spite of its good accuracy, DPSO still needs more improvement. Moreover, particles of the PSO-based MPPT in [17] are initialized around GP by means of Lagrange Interpolation Formula. This technique needs fewer iteration. But, the complexity of the PSO search is still high. GA and fuzzy logic approach are compared in [18],[28] for a grid-connected PV system. GA gives good performance. But, the validity of the proposed method is tested for only one shading pattern which is considered simple by using two series connected PV arrays. As a result, only two peaks are exhibited when PS occurs.

In the present paper, an improved version of the MPPT algorithm based on the Dynamic PSO previously tested by authors in [19], is proposed for a partially shaded grid-connected PV system for the purpose of enhancing its performance and reducing the convergence time. The proposed MPPT is used to extract the MPP under all operating states, especially when PV characteristics display more than two peaks. This work aims additionally to compare the algorithm here proposed with GA and P&O methods. In this context, the performances of different MPPT techniques are tested using the standard KC200GT PV generator by Matlab/Simulink tool under irradiance variation, then under PS. The grid side control is investigated as well through developing different control loops. The PID controllers of the PV system are tuned by GA which searches for the PID gains which optimizes the most the power transfer between the PV generator and the grid.

In the present study, the modelling of the PV generator is developed in section 2. PV curves under PS conditions are displayed. Different MPPT algorithms are briefly described in section 3. In section 4, the grid side modelling and control are developed. Simulation results of MPPT methods under various operating conditions are discussed in Section 5. Comparison and comments supporting the reliability and the robustness of the PSO algorithm are given. Finally, section 6 draws the conclusion followed by references.

2. Partially Shaded PV Generator

2.1. PV Generator modelling

The components of the considered PV conversion system are a PV generator, a DC/DC and the DC/AC converters, and the main grid. The principal mission of the chosen conversion system is to extract the maximum active power through the boost converter operating with a suitable MPPT and managing, as well, the active and reactive power injected into the grid via the inverter.

The EMR for all components are interconnected in order to frame the entire system EMR, with respecting the integral causality and following the action-reaction principle. MCS which allows the control loop modelling is deduced by inversion of the EMR [20]. The entire grid-connected PV system is shown in Fig.1.

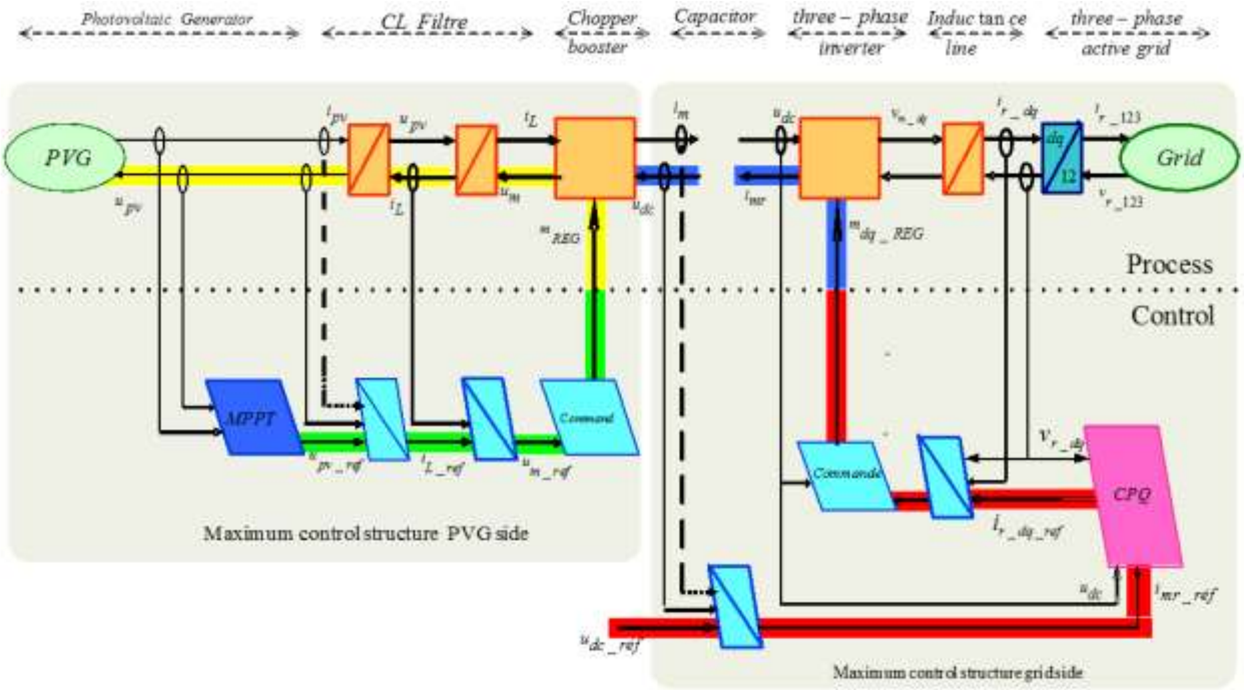

Fig. 1. The EMR and its reverse MCS of the entire system.

Among numerous existing PV array models, the single diode model is known to be usually explored for the solar cell modelling owing to its simplicity and accuracy, as displayed in Fig.2 [7],[29].

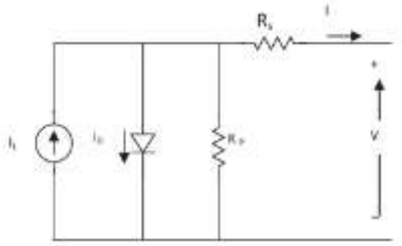

Fig. 2. Equivalent circuit model of a solar PV cell.

Eq. (1) describes the PV array modelling as shown below:

$$I_{pv}=N_p\left(I_{ph}-I_0\left(e^{\frac{V_{pv}+R_{sg}I_{pv}}{N_sV_T}}-1\right)\right)-\frac{V_{pv}+R_{sg}I_{pv}}{R_{shg}} \tag{1}$$

I_{ph} represents the photo current which is strongly dependent on temperature according to the Eq. (2):

$$I_{ph}=\left(\frac{G}{G_{STC}}\right)\left(I_{phn}+K_I\left(T-T_{STC}\right)\right) \tag{2}$$

The nominal photo current I_{phn} is determined by Eq. (3):

$$I_{phn}=\left(\frac{R_s+R_{sh}}{Rs}\right)I_{scn} \tag{3}$$

The diode reverse saturation current I_0 is deduced by the Eq. (4):

$$I_0=\frac{I_{scn}+K_I\Delta T}{\frac{I_{scn}+K_I\Delta T}{e^{aVt}}-1} \tag{4}$$

The PV module specifications are enumerated in Table 1. [21].

Table 1. Parameters of the used single PV module

Parameters	Value	Parameters	Value
I_{scn}	8.21	N_s	54
V_{ocn}	32.9	N_p	1
V_{mpp}	26.3	K_v	-0.123
I_{mpp}	7.61	K_I	0.0032

2.2. PV Generator characterization under Partial Shading

When the PV Generator is affected by PS, the power consumption is raised since the PV module under shade no longer acts as a power source but like a load. That's why a bypass diode is required in parallel with every PV module to protect the PV generator from hot spot phenomenon [21]. Figure.3 illustrates 3 series PV modules connected with 3 bypass diodes and one Blocking Diode. Among them, the third module is subjected to PS.

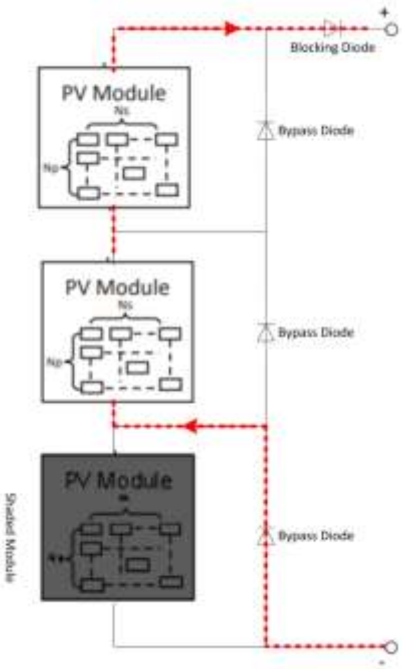

Fig. 3. PV Panel under partial shading

The PV characteristics exhibit usually a unique MPP for a single module when exposed to constant irradiance and temperature. The Power-Voltage (P-V) characteristic With no shading is depicted in Fig.4 at T=25°C and varying irradiance G.

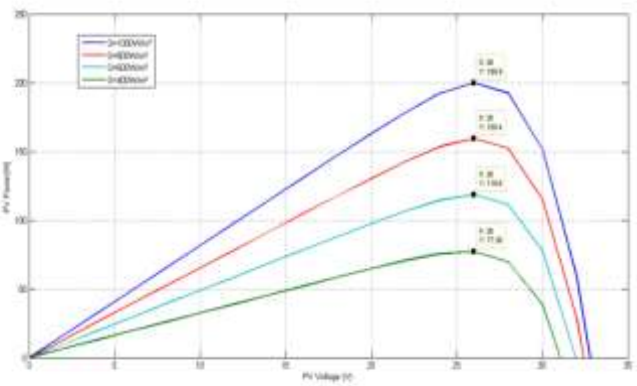

Fig. 4. P-V curve under varying irradiance**.**

However, the power curve will be distorted and exhibits multiple peaks as shown in Fig.5 for the P-V curve, and Fig.6 for the Current-Voltage (I-V) curve if the incident solar irradiation on the PV generator is not uniform due to a nearby tree, buildings, or even a cloud. According to [22], the P–V curve of PV generators consisting of k series PV modules exhibits at most k peaks.

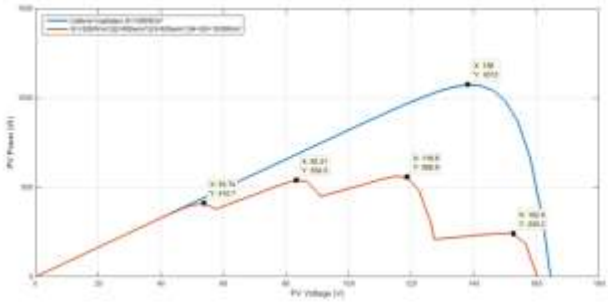

Fig. 5. P-V curve subjected to PS.

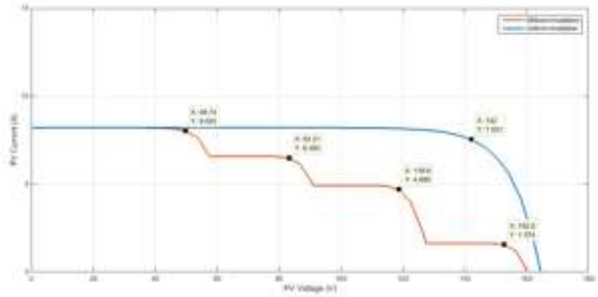

Fig. 6. I-V curve subjected to PS.

3. MPPT Algorithms for Partially Shaded PV Systems

The conventional algorithms usually fail to optimally amend the MPP for a PV array suffering from PS, hence, its usefulness diminishes rapidly [23], and a more accurate MPPT process is required for the purpose of continuously and optimally extract power. Among various techniques in the literature, PSO and GA algorithms suit well with MPPT search thanks to their simplicity and ability to discriminate between GP and local ones regardless of environmental variations [23].

3.1. Genetic Algorithm

This optimization technique is a population-based algorithm. It is a complete search scheme that depends on natural evolution process and originally introduced by Holland [24]. GA incorporates three main operators specifically the selection, crossover, and mutation and it relies on the survival of the fittest rule. During the selection procedure, a chromosome with higher fitness value is chosen from the present generation's population and included in the following one. A combination of two chromosomes is done during the crossover step and new children are created. The new offspring are assessed and incorporated into the population replacing the weaker candidates of the last generation. From that point onward, chromosomes are gone through a mutation procedure since it guarantees genetic variety and looks for the GA stochastic variability for speedier convergence [25].

By using GA, the chromosome position represents the required output voltage at every iteration. By means of Eq. (5) and Eq. (6), better offspring are generated Y(k) and Y(K+1) [26]:

$$Y(k) = r \times X(k) + (1-r) \times X(k+1) \quad (5)$$

$$Y(k+1) = (1-r) \times X(k) + r \times X(k+1) \quad (6)$$

$r \in [0,1]$

GA is continuously modified by reinitializing the first population after every detected abrupt irradiance variation to reach the new MPP. The algorithm is initialized when the following conditions are satisfied:

$$\left|V(k+1)-V(k)\right| < \Delta V \quad (7)$$

$$\left|\frac{P_{pv}(k+1)-P_{pv}(k)}{P_{pv}(k)}\right| > \Delta P \quad (8)$$

The following parameters are used for running the algorithm:

population number N_p=4;

$\Delta P=0.15$; $\Delta V=0.4$;

Crossover probability P_c=0.9;

3.2. Modified PSO-based MPPT

The PSO is an evolutionary algorithm which mimics the behavior of birds and used for solving the complex optimization problems [19]. First, a population is chosen and set into motion. Moves are made according to a relation exploiting the position and velocity of each candidate solution. Every particle position is determined according to the nearby best position (Pbest) and the global best (Gbest) position through the entire population. Every individual continues following the two positions until a predetermined ceasing criterion is reached (fitness function) or a maximum iteration number is reached. The following equations are used to update the velocity and position of each particle [19]:

$$v_j^{(k+1)} = \omega v_j^{(k)} + c_1^{(k)} r_1 (P_{best} - x_1^{(k)}) + c_2^{(k)} r_2 (G_{best} - x_2^{(k)}) \quad (9)$$

$$x_j^{(k+1)} = x_j^{(k)} + v_j^{(k+1)} \quad (10)$$

where the inertial weight; ω=0.9;
r_1 and $r_2 \in [0,1]$

Parameter selection phase: The reference voltage value which represents the perturbation signal obtained through the MPPT block, defines the particle position in the proposed system. The fitness function to be optimized is developed in Eq. (11). It represents the generated PV power in every iteration.

$$\text{Fitness}=Vpv*Ipv \quad (11)$$

The number of particles should be rigorously fixed since the larger number of particles is, the more accurate the GP tracking but the longer the computational time becomes. Thus, a compromise between good tracking speed and efficiency should be ensured. Consequently, a 4 sized population is chosen. This choice reduces the complexity and the tracking time of the system.

Initialization Phase: The population (PV Voltages) is initialized. The initial population is no longer randomly generated. PSO particles are placed on fixed positions with same distance. The population consists of 4 individuals which covers the search space and represented by the following vector:

$$[V_1 \quad V_2 \quad V_3 \quad V_4] = [0.2 \quad 0.4 \quad 0.6 \quad 0.8] * 5.Voc \quad (12)$$

Fitness Evaluation: The proposed algorithm aims to extract the maximum PV power under any circumstances, especially under PS. Indeed, the conversion scheme a feedback voltage loop as depicted in Fig.7. The resulted reference voltage V_{ref} is used for computing the error applied then to the entrance of a PID controller so as to generate the appropriate control signal for the converter. The fitness value P_{PV} is then calculated for the i_{th} particle of the population.

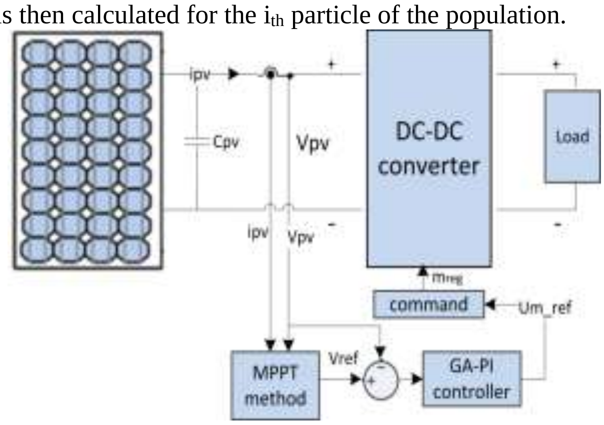

Fig. 7. MPPT control structure with feedback PV loop

Local and Global best position update: Whenever the fitness value of the i_{th} particle is greater than Pbest, the current value is replaced with the new P_{best} and G_{best} takes the value of the best fitness of all particles.

Velocity and position update: The proposed PSO algorithm main target is to prevent the divergence of the particles in the search space. To do so, the cognitive and social learning rate c_1 and c_2 respectively aren't taken as constants any more. The velocity and position are computed accordingly using the Eq. (13), Eq. (14), and Eq. (15) cited below:

$$v_j^{(k+1)} = \omega v_j^{k} + c_1 r_1 (P_{best} - x_1^{(k)}) + c_2 r_2 (G_{best} - x_2^{(k)}) \quad (13)$$

where

$$c_1 = (c_{1max} - c_{1min}) \frac{k}{n} + c_{1min} \quad (14)$$

$$c_2 = (c_{2max} - c_{2min}) \frac{k}{n} + c_{2min} \quad (15)$$

$c_{1min} = 2$ and $c_{1max} = 1$ the initial and final cognitive parameters respectively.

$c_{2min} = 1$ and $c_{2max} = 2$: the initial and final social parameters respectively.

The cognitive parameter is chosen to decrease linearly whereas the social parameter value is increasing linearly.

At every iteration, two sensors I_{pv}, and V_{pv} are extracted from the PV generator to the MPPT block to calculate the PV power as portrayed in Fig.7. The particle moves to the new position according to its fitness value with the updated velocity. Eq. (10) defines the updated position of the particle.

The generated reference voltage obtained through the MPPT block is used for computing the error applied then to the entrance of a PID controller so as to generate the appropriate control signal (U_{m_ref}). The PID parameters of the PV control loop are tuned by GA for a better MPP tracking. The m_reg is then obtained in order to drive the DC/DC converter. As well, the MPPT algorithm generates another reference signal which is varying continuously until the optimum point is achieved and tracks accurately the MPP under any circumstances.

4. Grid Side Modelling and Control

4.1. Grid side modelling

The PV generator pictogram delivers a current I_{PV} and receives by reaction with the system the DC bus voltage V_{pv} of the LC filter. DC/DC and DC/AC converters (based on Matrix Topology without energy storage) are modeled in average value (the switching functions are replaced by duty cycles) [27]. The capacitor C_{PV} is used for controlling the PV output voltage. It is modeled by means of the following equation:

$$C_{PV}\frac{dV_{pv}}{dt}+\frac{V_{pv}}{R}=i_{pv}-i_L \tag{16}$$

The inductor L is used to apply the source alternating rule. It can be modeled by the following differential equation:

$$L\frac{di_L}{dt}+r.i_L=V_{pv}-U_m \tag{17}$$

$$\begin{cases} u_m=m_{reg}\times u_{dc} \\ i_m=m_{reg}\times i_L \end{cases} \tag{18}$$

For the grid side modelling, a capacitor C_1 is connected to the DC link for the purpose of controlling the voltage applied to the input of the three-phase inverter and maintaining it equal to a preset value. The voltage across C_1 can be described by the following differential equation:

$$C_1\frac{du_{dc}}{dt}+\frac{u_{dc}}{R}=i_m-i_{mr} \tag{19}$$

The simple voltages and currents modulated by the inverter in the park reference can be expressed by:

$$\begin{cases} \begin{bmatrix} v_{md} \\ v_{mq} \end{bmatrix}=\frac{u_{dc}}{2}\begin{bmatrix} m_d \\ m_q \end{bmatrix} \\ i_{mr}=\frac{1}{2}\left(m_d i_{rd}+m_q i_{rq}\right) \end{cases} \tag{20}$$

$$\begin{bmatrix} v_{rd} \\ v_{rq} \end{bmatrix}=\left[P(\theta)\right]\begin{bmatrix} v_{r1} \\ v_{r2} \end{bmatrix} \tag{21}$$

$$\begin{bmatrix} i_{rd} \\ i_{rq} \end{bmatrix}=\left[P(\theta)\right]\begin{bmatrix} i_{r1} \\ i_{r2} \end{bmatrix} \tag{22}$$

where

$$\left[P(\theta)\right]=\sqrt{\frac{2}{3}}\begin{bmatrix} \cos(\theta) & \cos(\theta-2\pi/3) \\ -\sin(\theta) & -\sin(\theta-2\pi/3) \end{bmatrix}$$

(23)

$$(L_1\frac{d}{dt}+r_1)\begin{bmatrix} i_{rd} \\ i_{rq} \end{bmatrix}=\begin{bmatrix} v_{md} \\ v_{mq} \end{bmatrix}-\begin{bmatrix} v_{rd} \\ v_{rq} \end{bmatrix}+\begin{bmatrix} 0 & L_1\omega \\ -L_1\omega & 0 \end{bmatrix}\begin{bmatrix} i_{rd} \\ i_{rq} \end{bmatrix} \tag{24}$$

P and Q active and reactive powers respectively are computed using the conventional instantaneous power definition in *dq* system, as shown in Eq. (25):

$$\begin{bmatrix} P \\ Q \end{bmatrix}=\begin{bmatrix} v_{rd} & v_{rq} \\ v_{rq} & -v_{rd} \end{bmatrix}\begin{bmatrix} i_{rd} \\ i_{rq} \end{bmatrix} \tag{25}$$

The objective of this stage is to control the currents injected into the grid. It is needed then to determine the final drives and to be applied at the entrance of the three-phase inverter, according to Eq. (26):

$$\begin{cases} m_{d\_reg}=\dfrac{v_{md\_ref}}{u_{dc}} \\ m_{q\_reg}=\dfrac{v_{mq\_ref}}{u_{dc}} \end{cases} \tag{26}$$

The block diagram of the control method which includes the MPPT algorithm as well the current control of the inverter is illustrated in Fig.8.

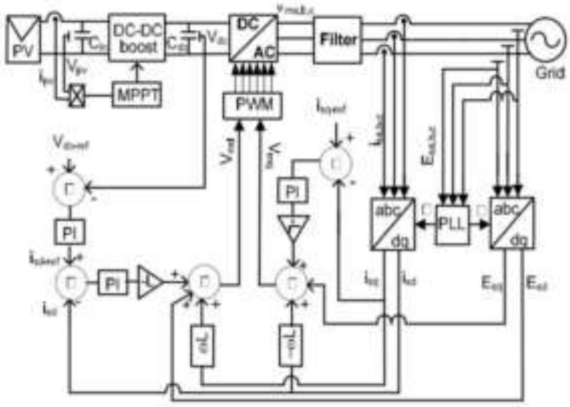

Fig. 8. Bloc diagram of the proposed control method

4.2. Genetic Algorithm-based Grid side control

The PID parameters of the grid side control loops are additionally tuned by GA as a part of this paper. GA searches for the three controller gains that guarantee the following targets: tight control of the DC voltage, conveying the desired yield power to the grid, and maintaining the unity power factor. In every control loop, the response of each chromosome which comprises of a set of PID gains is computed in the global system. Every chromosome must be assessed in each iteration by means of a Fitness Function which is required to assess the best PID parameters that convey the speediest rise time and the smallest overshoot [26].

The GA parameters listed in Table 1. are used for randomly generating the initial population (KP, KI, KD). Small population size is taken to enable the system response to be raised quickly.

Table 1. GA Parameters for tuning PID gains

Description	Parameters
N_p	20
$iter_{max}$	100
P_c	0.5
P_m	0.01

5. Simulation of the Proposed System

The studied system comprises 5 series PV modules, each one of them consists of 54 serial cells delivering under uniform irradiation 1kW. Challenging tests verifying the reliability of the tracking performance of the developed MPPT have been carried out. A comparison is made between the PSO, GA, and P&O under fast changing irradiance, and under partial shading.

Results of simulation of the above algorithms are performed under the same following conditions:

P=1kW, C=220µF, R=100kΩ, L=23mH, C_1=5000µF, R_1=10kΩ, r_1=0.0002Ω, L_1=1mH, U_r=380V, f=50Hz.

5.1. MPPT responses under fast varying irradiance

The irradiation can quickly change by environmental conditions. Five irradiation step signals were simulated. The scenario of the irradiance variation is given through Fig.9.

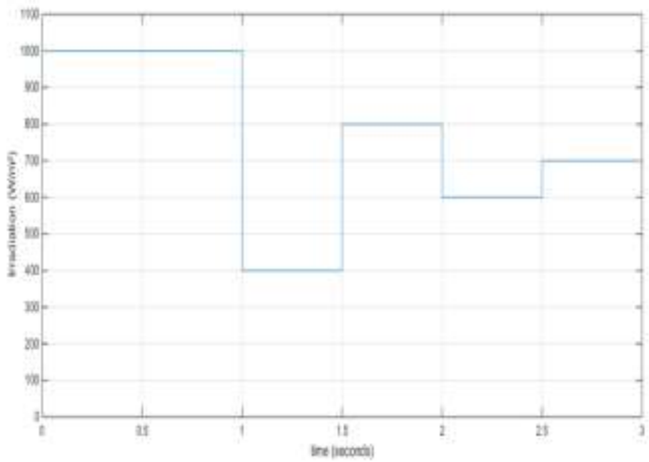

Fig. 9. Illumination variation

In this test, the five series-connected PV generators are initially exposed to uniform illumination (1000W/m²) and constant temperature is 25°C. The generated PV Power reaches 1kW. Figure. 10 shows the response of the tracked power. Under fast-changing irradiation, it is evident from simulation results in fig. that the three techniques have successfully reached the maximum available power at every irradiation step change. Thus, the ability of MPP tracking is demonstrated for the three methods. For t=[0 1s], the PV power almost reaches 1kW under STC, by using P&O technique, which corresponds to the MPP. However, the convergence speed toward the MPP is relatively low as compared to PSO and GA.

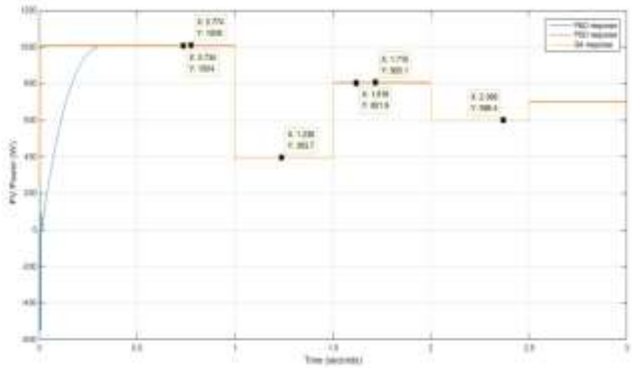

Fig. 10. PV Power tracking curves under fast changing irradiation

Then, under constant temperature, when a step change of irradiance happens, it can be observed that the three MPPT techniques have close results and always succeed to extract the MPP. Furthermore, in the case of P&O, a full scan of the PV curves is required before the MPP is reached which leads to a significant energy loss as portrayed in Fig.11. Under fast changing irradiation, PSO and GA perform in like manner and the accurate MPP is reached in every irradiation step change with fewer fluctuations and shorter time.

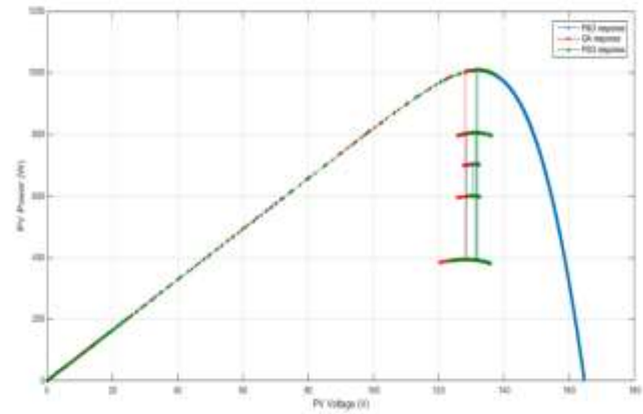

Fig. 11. P-V curve under fast changing irradiation

5.2. MPPT responses under partial shading

Simulations are conducted under three challenging shading profiles applied to a 5S configuration for the purpose of verifying further the improvement of MPPT performances. The first two different shading templates are portrayed in Fig.12 (a) and (b), two different resulted PV curves are depicted in Fig.12 (c).

The tracking results are depicted in Fig.13 and Fig.14 for pattern 1 and 2 respectively. Considering the first template, the P-V curve is made up of five peaks with 408.8W as the GP whereas the P-V curve of pattern 2 exhibits 5 peaks with 267.5W as the GP. The proposed PSO-based MPPT is capable of extracting the maximum power with 0.02s for both cases. However, by examining the tracking curves of GA in Fig.13 and Fig.14, it is worthy to note that the

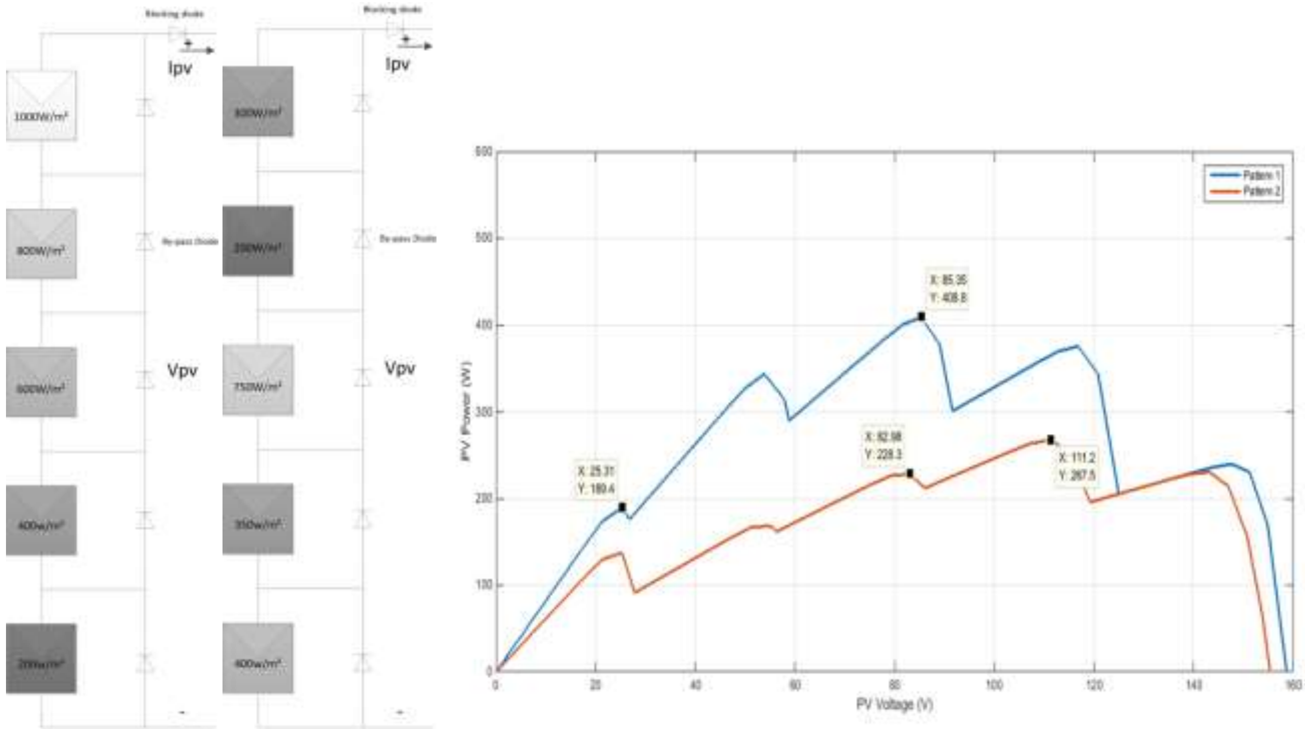

(a) (b) (c)

Fig. 12 5S configuration under PS: (a) Template 1, (b) Template 2, and (c) P-V characteristics

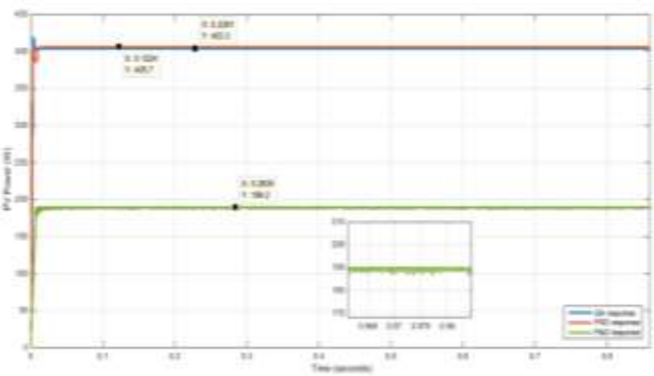

Fig. 13. PV Power tracking curves for template 1

convergence speed towards the GP varies from one pattern to another. This fact is due to the stochastic behavior of the GA and the randomly generated solutions. Indeed, although the GP is successfully reached for the first pattern (403.3W), GA remains stuck in a local maximum in the second pattern (246.4W) with more oscillation and higher transient time. The P&O algorithm fails to converge to the GP and ceases in local maxima (P=189.2W for pattern 1 and P=227.8W for pattern 2). Besides, it produces oscillations in the steady state because of the perturbation signal around the MPP. Similarly, in the case of template 2, only the proposed PSO-based MPPT is able to harvest the GP under PS with less oscillation and transient time.

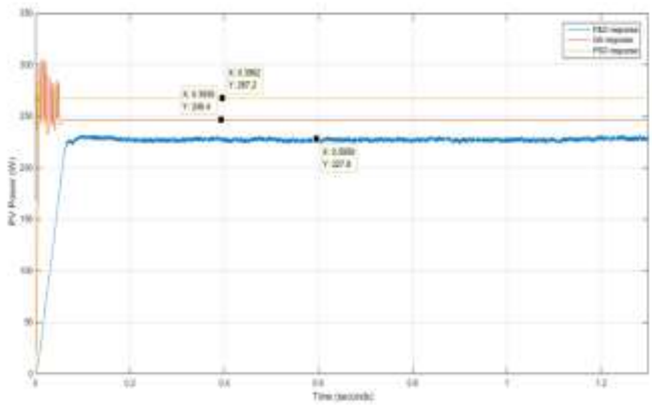

Fig. 14. V Power tracking curves for template 2

Another more arduous shading template is experienced on the 5S configuration which is given by Fig.15. In this case, PV modules M2, M3 receive different varying irradiation while M1, M4 and M5 receive a constant irradiation of 1000W/m². The present study is carried out to compare the transient responses of the three MPPT techniques when shading pattern changes from one to another. Four different shading configurations are feasible.

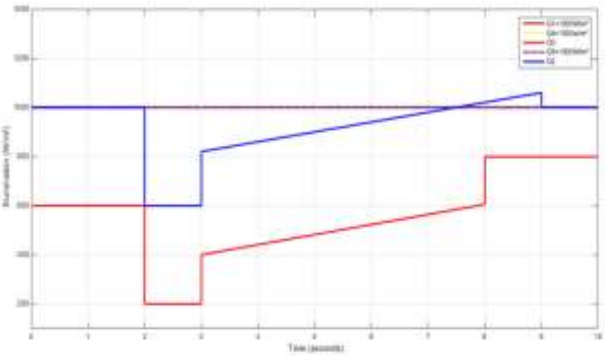

Fig. 15. Illumination variation of template 3

The first shading step of the considered template is made to exist for 2s and the resulted P-V curve has 2 peaks. For the other shading steps, 5 peaks are displayed and the GP is varying according to illumination variation in the second and the third PV modules. The tracking curves for each method are displayed in Fig.16. The comparison between different MPPT methods highlight the superiority of the proposed algorithm since it is likely to reach GP in every step change. Besides, its immediate reaction to any power variation caused by PS is also demonstrated. However, P&O settles always to local maxima and the search process requires longer time interval which reduces the conversion efficiency. Further, GA gives promising results but the exact MPP hasn't been reached and the GA response remains too close to the operating point.

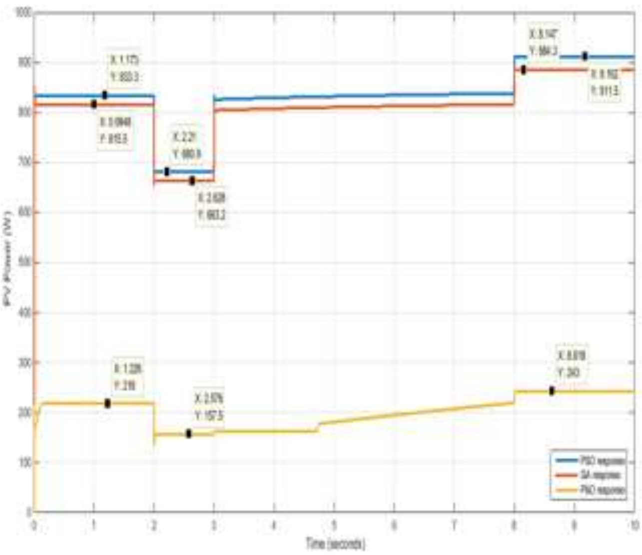

Fig. 16. PV Power tracking curves for template 3

Because of PS, the mismatch loss (MML) is obtained by the following equation :

$$MML(\%) = \frac{Maximum\ power\ of\ PV\ system}{\sum_{i=1}^{N} P_{\max(i)}} * 100 \qquad (27)$$

The MML percentage reflects the generated power rate. The more the MPPT technique succeeds the GP tracking, the higher the generated power rate will be.

Performances of MPPT methods applied to the 5S PV array are compared in Table 2. The proposed PSO algorithm usually achieves the GP when compared to either GA or P&O techniques. This leads to extracting the maximum PV power output with least time resulting in more MML. Since the GP is attained faster by using PSO method, the MML and the tracking efficiency are also higher. The numerical data clearly highlight the supremacy of the PSO algorithm.

5.3. Grid Side Control

The aim of the GA based PID control consists in obtaining a tight control of the DC link voltage and keeping it constant independently of the power variation during the threefold PS templates. PSO technique is adopted for the rest of the paper thanks to its better performances. Fig.17 validates the DC link voltage control which ensures the perfect follow-up between the reference and the measured dc link voltage when the system experiences arduous climatic changes. The DC link voltage is permanently sustained at 700V even when PS occurs, except the small perturbations at every illumination variation as figured in Fig.17(c).

Table 2. Performance comparison of MPPT methods under PS.

Sha-ding Tem-plate	Tra-cking Me-thods	Po-wer (W)	MPP from P-V curve	Tra-cking speed (s)	% Tra-cking efficien-cy	%Mis-match Power Loss (MML)
1	PSO	405.7	408.8	0.02	99.24	26.05
	GA	403.3		0.01	98.65	25.9
	P&O	189.2		0.02	46.28	12.15
2	PSO	267.2	267.5	0.01	99.88	25.9
	GA	246.4		0.06	92.11	23.88
	P&O	227.8		0.08	85.15	22.07

Figure.18 represents the injected grid currents after using PSO optimization technique under different climatic conditions. GA-PID controller seems to be effective in the steady state and keeps delivering the desired output power to the grid with unity power factor. Table 3. enumerates the controller gains of the system control loops.

Table 3 . Controller parameters

Parameters	P	I	D
PV voltage loop	0.2797	0.0983	0
DC link voltage loop	1.1270	0.0871	0
Grid current loops	6.1386	0.3625	0

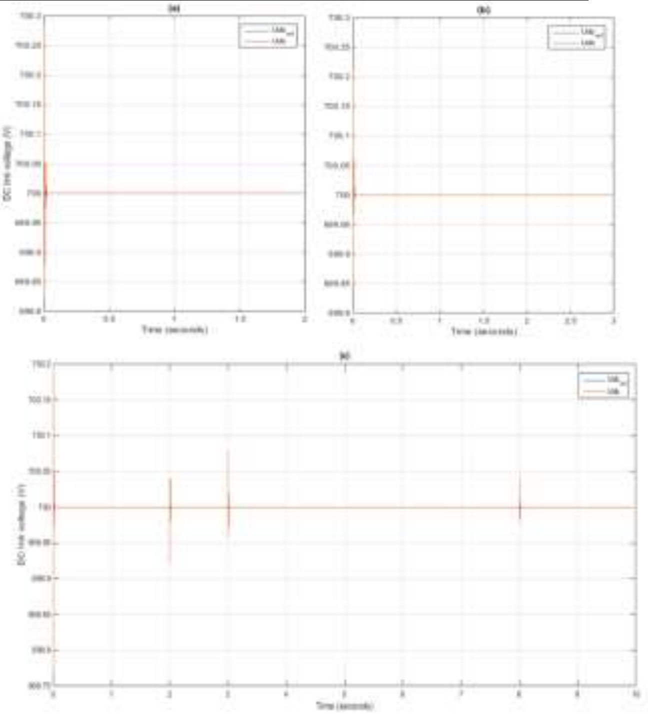

Fig. 17. DC link Voltage and its reference under different shading conditions: (a) Template 1, (b) Template 2, and (c) Template 3

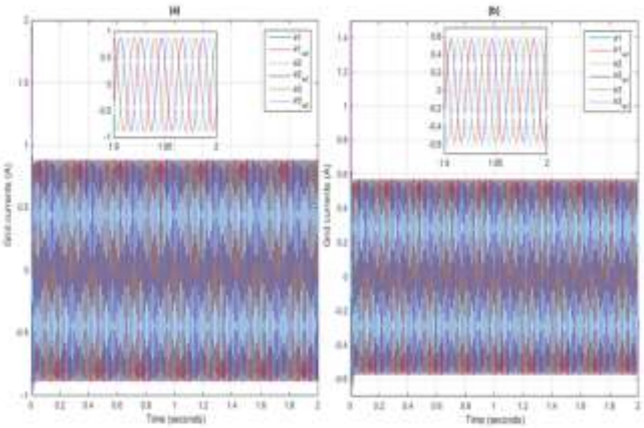

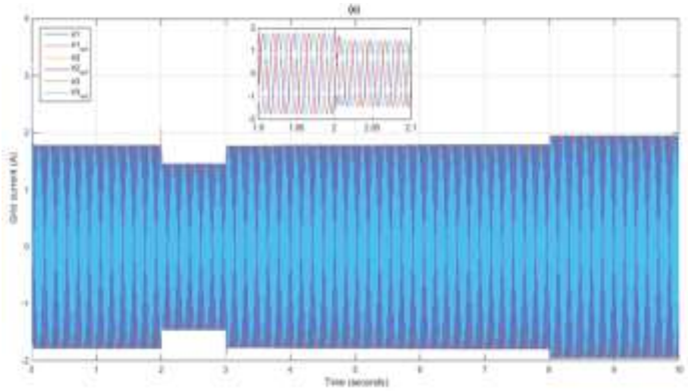

Fig. 18. Grid current under partial shading: (a) template 1, (b) Template 2, and (c) Template 3

6. Conclusion

The present paper proposes a new MPPT technique based on Dynamic PSO (DPSO), a variant of the standard PSO technique. A comparative assessment of three MPPT algorithms, namely the proposed PSO, GA, and P&O for grid-connected PV systems. These techniques are employed to detect the global MPP under any circumstances, especially when the PV generator suffers from PS. Under shade, the new method seems to be reasonable to be used for tracking the MPP and a good tradeoff between simplicity, speed, and efficiency. P&O technique, however, cannot be employed since the global maximum cannot be reached. Furthermore, the used variant of PSO outperforms the other methods conditions for the following reasons:

1. Only two sensors (V_{pv}, I_{pv}) are required for the MPP global search.

2. Under PS conditions, thanks to the initial fixed population and the new setting of the cognitive and social learning rate c_1 and c_2 respectively, the convergence is assured when the system presents a multi extreme MPP problem caused by partial shading challenging scenarios.

3. The reference voltage (V_{ref}) value which represents the perturbation signal, is obtained through the MPPT block instead of the duty cycle.

4. The generated reference voltage is used for computing the error applied to the entrance of a PID controller so as to control the converter. The PID parameters of the PV control loop are tuned by GA for a better MPP tracking.

Moreover, the GA based PID control is proposed for controlling the cascade loops of the grid side in order to deliver the desired output power to the grid. Simulations are executed by means of Matlab/Simulink to conclude that DPSO algorithm defeats GA and P&O.

The authors are intending to develop an experimental prototype of the designed PSO and improving it through developing a new variant of PSO based on hybrid PSO for the purpose of reducing the searching area.

References

[1] M. A. Green, “Photovoltaic principles,” in Physica E: Low-Dimensional Systems and Nanostructures, 2002, vol. 14, no. 1–2, pp. 11–17.

[2] B. Veerasamy, W. Kitagawa, and T. Takeshita, “MPPT method for PV modules using current control-based partial shading detection,” in 3rd International Conference on Renewable Energy Research and Applications (ICRERA), pp. 359–364, 2014.

[3] B. Veerasamy, A. R Thelkar, G. Ramu, and T. Takeshita, "Efficient MPPT control for fast irradiation changes and partial shading conditions on PV systems," In Renewable Energy Research and Applications (ICRERA), 2016 IEEE International Conference, pp. 358-363, IEEE, November 2016.

[4] R. Boukenoui, R. Bradai, A. Mellit, M. Ghanes and H. Salhi, 'Comparative Analysis of P&O, Modified Hill Climbing-FLC, and Adaptive P&O-FLC MPPTs for Microgrid Standalone PV System', 4th International Conference on Renewable Energy Research and Application (ICRERA), Palermo, Italy, pp. 1095-1099, Nov 22-25, 2015.

[5] Abdourraziq, M. A., Ouassaid, M., Maaroufi, M., & Abdourraziq, S. (2013, October). Modified P&O MPPT technique for photovoltaic systems. In Renewable Energy Research and Applications (ICRERA), 2013 International Conference (pp. 728-733). IEEE.

[6] D. Sera, T. Kerekes, R. Teodorescu, and F. Blaabjerg, “Improved MPPT algorithms for rapidly changing environmental conditions,” in EPE-PEMC 2006: 12th International Power Electronics and Motion Control Conference, Proceedings, 2007, pp. 1614–1619.

[7] S. Krim, S. Gdaim, A. Mtibaa and MF. Mimouni, “FPGA Contribution in Photovoltaic Pumping Systems: Models of MPPT and DTC-SVM Algorithms,” International Journal of Renewable Energy Research (IJRER), 6(3), 866-879, 2016.

[8] A. K. Rai, N. D. Kaushika, B. Singh, and N. Agarwal, “Simulation model of ANN based maximum power point tracking controller for solar PV system,” Sol. Energy Mater. Sol. Cells, vol. 95, no. 2, pp. 773–778, 2011.

[9] B. N. Alajmi, K. H. Ahmed, S. J. Finney, B. W. Williams, and B. Wayne Williams, “A maximum power point tracking technique for partially shaded photovoltaic systems in microgrids,” IEEE Trans. Ind. Electron., vol. 60, no. 4, pp. 1596–1606, 2011.

[10] L. L. Jiang, D. L. Maskell, and J. C. Patra, “A novel ant colony optimization-based maximum power point tracking for photovoltaic systems under partially shaded conditions,” Energy Build., vol. 58, pp. 227–236, 2013.

[11] X. S. Yang, “A new metaheuristic Bat-inspired Algorithm,” in Studies in Computational Intelligence, 2010, vol. 284, pp. 65–74.

[12] L. Zhou, Y. Chen, K. Guo, and F. Jia, “New approach for MPPT control of photovoltaic system with mutative-scale dual-carrier chaotic search,” IEEE Trans. Power Electron., vol. 26, no. 4, pp. 1038–1048, 2011.

[13] K. Ishaque, Z. Salam, M. Amjad, S. Mekhilef, “ An improved particle swarm optimization (PSO)-based MPPT for PV with reduced steady-state oscillation”, IEEE Trans Power Electron, vol. 27, no. 8, pp. 3627–38, 2012.

[14] J. Ahmed and Z. Salam, “A Maximum Power Point Tracking (MPPT) for PV system using Cuckoo Search with partial shading capability,” Appl. Energy, vol. 119, pp. 118–130, 2014.

[15] Y. H. Ji, D. Y. Jung, J. G. Kim, J. H. Kim, T. W. Lee, and C. Y. Won, “A real maximum power point tracking method for mismatching compensation in PV array under partially shaded conditions,” IEEE Trans. Power Electron., vol. 26, no. 4, pp. 1001–1009, 2011.

[16] K. Ishaque and Z. Salam, “A Deterministic Particle Swarm Optimization Maximum Power Point Tracker for Photovoltaic System under Partial Shading Condition,” IEEE Trans. Ind. Electron., vol. 60, no. 8, pp. 1–1, 2012.

[17] R. Koad, A. F. Zobaa, and A. El Shahat, “A novel MPPT algorithm based on particle swarm optimisation for photovoltaic systems,” IEEE Trans. Sustain. Energy, vol. 8, no. 2, pp. 468–476, 2016.

[18] M. Ben Smida and A. Sakly, “A comparative study of different MPPT methods for grid-connected partially shaded photovoltaic systems,” International Journal of Renewable Energy Research.(IJRER), vol. 6, no. 3, 2016.

[19] A. Badis, M. Boujmil, M. Mansouri, “ A Comparative Study on Maximum Power Point Tracking Techniques of Photovoltaic Systems”, International Journal of Energy Optimization and Engineering, vol. 7, no. 1, pp. 66-85, 2018.

[20] W. Lhomme , P. Delarue , F. Giraud , B. Lemaire-Semail , A. Bouscayrol , “ Simulation of a Photovoltaic Conversion System using Energetic Macroscopic Representation”, 15th International Power Electronics and Motion Control Conference (EPE/PEMC), Novi Sad, Serbia, pp. DS3e-7, 4-6 September, 2012.

[21] A. Dolara, F. Grimaccia, M. Mussetta, E. Ogliari, and S. Leva, “An evolutionary-based MPPT algorithm for photovoltaic systems under dynamic partial shading,” Appl. Sci., vol. 8, no. 4, 2018.

[22] P. Lei, Y. Li, and J. E. Seem, “Sequential ESC-based global MPPT control for photovoltaic array with variable shading,” IEEE Trans. Sustainable Energy, vol. 2, no. 3, pp. 348–358, Jul. 2011.

[23] K. Ishaque , Z. Salam , “ A review of maximum power point tracking techniques of PV system for uniform insolation and partial shading condition”, Renewable

and Sustainable Energy Reviews, vol. 19, pp. 475–88, 2013.

[24] J. Holland, “ Outline for a Logical Theory of Adaptive Systems”, Journal of the ACM, vol. 9, no.3, pp. 297-314, 1962.

[25] S. Hadji , J.G. Fateh, “ Genetic algorithms for maximum power point tracking in photovoltaic systems Keywords”, Proceedings of World Academy of Science Engineering and Technology, pp. 1–9, October 2011.

[26] A. Badis, M.N. Mansouri, and A. Sakly, “ PSO and GA-based maximum power point tracking for partially shaded photovoltaic systems”, 7th International Renewable Energy Congress (IREC 2016), Hammamet, Tunisia, pp. 1-6, 22-24 March 2016.

[27] A. Badis , M.N. Mansouri , and M.H. Boujmil ,“ A genetic algorithm optimized MPPT controller for a PV system with DC-DC boost converter”, International Conference on Engineering & MIS (ICEMIS), Monastir, Tunisia, pp. 1–6, 8-10 May 2017.

[28] S. Choudhury, P.K.Rout, “Adaptive Fuzzy Logic Based MPPT Control for PV System under Partial Shading Condition” International Journal of Renewable Energy Research (IJRER), Vol.5, No.4, 2015.

[29] A. Parisi, L. Curcio, V. Rocca, S. Stivala, A. C. Cino, A. C. Busacca, G. Cipriani, D. La Cascia, V. Di Dio, and R. Miceli, “Photovoltaic module characteristics from CIGS solar cell modelling,” in Proceedings of 2013 International Conference on Renewable Energy Research and Applications (ICRERA), pp. 1139–1144, 2013.